data to estimate the contribution of LiCl, we have determined that for pure DMAc $\delta_1 \sim 9 \pm 0.5$. Following the approach indicated above we obtained $\chi_{12} \sim 5.0$ and $\chi_{13} \sim 0.5$, which would be in line with Hsu and Prausnitz data assuming that LiCl played a comparable salting-in role on the two polymers. The assumption $\chi_{12} > \chi_{13}$ would tend to reduce the difference between the critical concentration for incompatibility evaluated above.

A final comment concerns the comparison of the present results with those obtained[4,5] for systems composed of two rigid polymers and a solvent. The latter systems exhibited a coexistence of three phases within the region corresponding to the biphasic gap of the two polymers. When above $v_2' = 0.065$ (0.08) the mesophase of cellulose I (L) in DMAc + 7.8% LiCl appears (Figures 3 and 4), we would have expected a region of coexistence of an isotropic and an anisotropic cellulose solution. The width of the biphasic gap was estimated in ref 14 to be $v_2''/v_2' \sim 1.32$ for a sample of regenerated cellulose II with DP = 288. However, it was also shown[14] that the solubility line encroached the biphasic gap, particularly when DP increased. Therefore, we believe that the anisotropic phase of cellulose observed here is not a pure phase. The separation of its components would require more extensive equilibration and problematic[14] centrifugation. Recognition of the biphasic nature of the anisotropic "phase" might not pose the same constraints to the variance of the system, as observed with the systems composed of two rigid polymers.[4,5] Here, in fact, the diluent is strictly a two-component system, although a large LiCl disproportion was not observed. For a truly three-component system, invariant compositions should prevail within the region of coexistence of three phases[4,5] (shadowed area in Figure 4). The data for the low molecular weight cellulose sample (Figure 4) are not inconsistent with this expectation, but a large deviation is exhibited by the system illustrated in Figure 3. Failure to achieve complete equilibration might be involved.

The observation that a mesogenic and a flexible polymer are incompatible not only by virtue of the entropy effect considered in Flory's theory[1,2] but also by virtue of the unfavorable interaction evidenced here enormously complicates the possibility of preparing desirable composites of the two polymers. The copolymerization route would appear a more promising approach.

**Acknowledgment.** This investigation was supported by the Italian Research Council, project "Chimica Fine e Secondaria".

## References and Notes

(1) Bianchi, E.; Ciferri, A.; Conio, G.; Marsano, E.; Tealdi, A. *Macromolecules* **1984**, *17*, 1526. Bianchi, E.; Ciferri, A.; Tealdi, A. *Ibid.* **1982**, *15*, 1268.
(2) Flory, P. J. *Ibid.* **1978**, *11*, 1138. Matheson, R. R.; Flory, P. J. *Ibid.* **1981**, *14*, 954.
(3) Paul, D. R.; Newman, S., Eds. "Polymer Blends"; Academic Press: New York, 1978; Vol. I.
(4) Marsano, E.; Bianchi, E.; Ciferri, A. *Macromolecules* **1984**, *17*, 2886.
(5) Marsano, E. *Polymer*, in press.
(6) Abe, A.; Flory, P. J. *Macromolecules* **1978**, *11*, 1122.
(7) Bianchi, E.; Ciferri, A.; Conio, G.; Lanzavecchia, L.; Terbojevich, M. *Macromolecules*, following paper in this issue.
(8) Kamide, K.; Miyazaki, Y.; Abe, T. *Polym. J. (Tokyo)* **1979**, *11*, 523.
(9) Kamide, K.; Saito, M. *Ibid.* **1962**, *14*, 517.
(10) Kamide, K.; Saito, M.; Abe, T. *Ibid.* **1981**, *13*, 421.
(11) Terbojevich, M.; Cosani, A.; Conio, G.; Ciferri, A.; Bianchi, E. *Macromolecules* **1985**, *18*, 640.
(12) Marx, M. *Makromol. Chem.* **1955**, *16*, 157. Marx-Figini, M.; Schulz, G. V. *Ibid.* **1962**, *54*, 102. Brandrup, J.; Immergut, E. M., Eds. "Polymer Handbook"; Wiley: New York, 1975; V-107.
(13) Turbak, A. F.; El-Kafrawy; Snyder, F. W.; Auerbach, A. B. UK Pat. Appl. GB 2055-107 A, 1981.
(14) Bianchi, E.; Ciferri, A.; Conio, G.; Cosani, A.; Terbojevich, M. *Macromolecules* **1985**, *18*, 646.
(15) Yamakawa, H.; Fujii, M. *Ibid.* **1974**, *7*, 128.
(16) Brant, D. A.; Goebel, K. D. *Ibid.* **1972**, *5*, 536.
(17) Flory, P. J. *Adv. Polym. Sci.* **1984**, *59*, 1.
(18) Barton, A. "Handbook of Solubility Parameters and Other Cohesion Parameters"; CRC Press: Boca Raton, FL, 1983.
(19) Hsu, C. C.; Prausnitz, J. M. *Macromolecules* **1974**, *7*, 320.

# Mesophase Formation and Chain Rigidity in Cellulose and Derivatives. 5. Cellulose Acetate in *N,N*-Dimethylacetamide

**E. Bianchi, A. Ciferri,* G. Conio,† L. Lanzavecchia,‡ and M. Terbojevich§**

*Istituto di Chimica Industriale, Università di Genova, Genoa, Italy.* *Received June 5, 1985*

ABSTRACT: The critical volume fraction for mesophase formation, $v_2'$, was determined in *N,N*-dimethylacetamide for fractions of a cellulose acetate with DS = 2.3. The triacetate and the monoacetate did not exhibit a mesophase. The occurrence of a biphasic region was demonstrated. $v_2'$ attains a limiting value of 0.33 at room temperature and increases with temperature, but encroachment with the solubility line prevents the observation of the $T_{NI}^0$ temperature for the pure polymer. Diluted solution data allow an evaluation of the persistence length, $q$, of the diacetate, which is 70 Å at 25 °C, and $d \ln q/dT = -7.8 \times 10^{-3}$ deg$^{-1}$. Light-scattering data reveal the occurrence of a small degree of association in moderately concentrated solutions. These results, and those previously obtained with other systems, are analyzed to derive final conclusions concerning the molecular interpretation of mesophase formation. $v_2'$ and the thermotropic effects are definitively correlated with chain rigidity, and association effects play only a minor role. Almost all features of the limiting behavior of semirigid mesogens are described by theory. However, a discrepancy on the absolute value of the limiting $v_2'$ remains, for which, however, several justifications can be advocated. A successful theory for the overall behavior of semirigid mesogen is not yet available.

The first two papers of this series dealt with the relationship between chain rigidity and mesophase formation for hydroxypropyl cellulose (HPC) in *N,N*-dimethylacetamide (DMAc)[1] and in dichloroacetic acid (DCA).[2] In parts 3 and 4 we investigated the relationship between aggregation and mesophase formation for cellulose in DMAc + LiCl.[3,4] In the final part of this series, we study chain rigidity and mesophase formation for cellulose acetates, with varying degrees of substitution, in DMAc.

Several investigations have dealt with the mesophase

† Centro Macromolecole Sintetiche e Naturali, CNR, Genoa, Italy.
‡ Thesis submitted to the University of Genoa for the Doctoral degree in Chemistry.
§ Centro Studi Biopolimeri, CNR, Padua, Italy.

0024-9297/86/2219-0630$01.50/0 

**Table I**
**Characteristics of Samples Investigated**

| sample | producer | DS | | $[\eta]^{25}_{DMAc}$, dL/g | $\bar{M}_v$[e] | $\bar{M}_w$ | $B \times 10^3$, mol·mL·g$^{-2}$ | $\langle R_G^2 \rangle^{1/2}$, Å |
|---|---|---|---|---|---|---|---|---|
| | | NMR[a] | titration[b] | | | | | |
| cellulose acetate A | Fluka Buchs SG triacetate | 2.67 | 2.84 | 2.63 | 214 000 | 165 000 | 0.7 | 360 |
| cellulose acetate B | Eastman Kodak 4655 DS = 2.46 | 2.25 | 2.30 | 1.90 | 115 600 | 112 000 | 0.7 | 330 |
| cellulose acetate C | Courtanz DS = 2.5 deacetylated[c] | | 0.9 | 1.74[d] | 86 000 | | | |

[a] $^1$NMR by Istituto Scientifico Chimica e Biochimica "Giuliano Ronzoni", Milan. [b] Titration of excess HCl following treatment with EtOH, NaOH, and HCl; ref 14. [c] Deacetylation by Novaceta di Magenta, Milan, using 0.75 N NaOH for 1 h. [d] Obtained from DMAc + 3%, 1%, 0.5%, and 0.1% LiCl and extrapolating to $C_s = 0$. [e] Using eq 1–3 for A–C, respectively.

behavior of CA. Meeten and Navard,[5] using cellulose triacetate in trifluoroacetic acid, concluded that the phase diagram does not contain a biphasic region where the isotropic and the cholesteric phase coexist. In our own study[6] of the ternary system CA/HPC/DMAc we were also unable to isolate the conjugated phases. However, the ternary diagram could be interpreted by assuming that a biphasic gap existed, but the phase separation was made difficult by the high viscosity ($\eta \sim 80\,000$ P) of the mixtures. Dayan et al.[7] also did not separate the two phases. However, they reported viscosity–concentration curves exhibiting a maximum and a minimum, a behavior similar to that observed with other mesogens in the biphasic region.

The interpretation of mesophase formation for CA is also affected by contradictions. Meeten and Navard[6] suggested that a coil → helix transition explains the formation of the mesophase above a critical polymer volume fraction $v_2'$. Dayan et al.[7] interpreted their data for CA in various solvents using lattice theories. However, they used an earlier theory[8] for semiflexible chains, the unsuitability of which has been recently discussed by Flory.[9] Patel and Gilbert,[10] working with cellulose triacetate in mixed solvents, used a virial theory without a knowledge of the persistence length, which is the central parameter of the theory.

Dilute-solution data for CA in DMAc have been reported by Kamide et al.[11,12] These reveal no aggregation effects of the type observed for cellulose.[3] However, association effects in relatively concentrated solutions have not been investigated.

## Experimental Section

**Materials and Solutions.** Three samples of cellulose acetate having DS between 2.67 and 1 were used. DS was determined by proton NMR[13] and by standardized chemical analysis (Table I).[14] Values obtained (Table I) are somewhat smaller than reported by the producer. Sample C was obtained by deacetylation of a sample with DS = 2.5 (Table I). Sample B was fractioned by successive solutional fractionation as described by Kamide et al.[11] The method is reported to yield fractions differing in molecular weight but not in DS. The polymer was exposed to an acetone/ethanol mixture and, after 24-h stirring at 25 °C, the of LiCl is added. Stirring is continued until the mixture is cooled supernatant was separated. The extracted polymer yielded the first fraction upon evaporation. The procedure was repeated on the undissolved polymer with increasing amounts of acetone in the mixture until the fractions included in Table II were obtained. DMAc was produced by Carlo Erba (RPE, Analyticals) and was treated with molecular sieves to remove traces of water. Solutions of samples with large DS (A and B) could be prepared by simply adding a known amount of polymer (dried under vacuum at 50 °C for 12 h) to a known amount of DMAc and stirring for several hours depending upon the concentration $C_p$. The latter is given as grams of polymer per 100 g of solution. Sample C, with the lowest DS, was not readily soluble in pure DMAc. To dissolve this sample we followed an approach similar to that employed for cellulose in DMAc/LiCl.[3,4] Weighted amounts of CA and DMAc are heated to the reflux temperature for 20 min. The mixture is allowed to cool to ~100 °C, and a weighted amount of LiCl is added. Stirring is continued until the mixture is cooled to room temperature. With 3% LiCl, the solubility limit for sample C was $C_p \sim 8\%$. Once solubilization was achieved, the amount of LiCl could be reduced by dilution with DMAc.

**Dilute Solutions.** Intrinsic viscosity was determined by using suspended-level Ubbelhode viscometers (solvent flow time > 100 s) in the concentration range 0.18–0.615 g/100 mL. Measurements were performed at $T = 25 \pm 0.05$ °C, but for sample B and its fractions, $[\eta]$ was also measured at 50, 70, and 110 °C in order to derive the temperature dependence of the persistence length. Molecular weights were obtained by using the following relations. For the triacetate[11]

$$[\eta] = (2.64 \times 10^{-4}) M_v^{0.75} \quad (1)$$

and for the diacetate[12]

$$[\eta] = (1.34 \times 10^{-4}) M_v^{0.82} \quad (2)$$

These relationships were obtained by Kamide et al. for samples dissolved in DMAc and having DS = 2.92 and 2.46, respectively. Kamide et al.[15] and Saito[16] also determined the $[\eta]$–$M_v$ relationship in DMAc for DS = 1.75 and DS = 0.49, the latter being

$$[\eta] = (19 \times 10^{-4}) M_v^{0.6} \quad (3)$$

According to our data, however, CA with DS < 1 should not be soluble in pure DMAc. We have nevertheless used eq 3 for sample C, obtaining the value of $[\eta]$ in pure DMAc by extrapolating the variation of $[\eta]$ with LiCl content ($C_s$) starting from a stock solution with $C_p = 2.99\%$ (w/w) and $C_s = 3.4\%$ (w/w). Light-scattering measurements were performed as described[3] in part 3 by using samples A and B and a Sofica Model 4200 photometer at $\lambda = 546$ nm and $T = 25$ °C. $dn/dc$ was found equal to 0.045 mL/g (Kamide et al. report 0.0418 for the diacetate[12] and 0.0398 for the triacetate[11] at $\lambda = 436$ nm). Solutions and solvents were clarified by centrifugation at 17 000 rpm for 2.5 h. Some solutions were later subjected to more extensive centrifugation to remove traces of associated species.

**Concentrated Solutions.** Polymer concentration was increased up to the solubility limit. In some cases the latter was verified by increasing the temperature to achieve dissolution and observing the reappearance of the solid on cooling. When a cholesteric mesophase was present, the critical concentration $C_p'$ at which the mesophase appears was determined by optical microscopy and sometimes by ORD, as described elsewhere.[1-4] The value of the critical polymer volume fraction, $v_2'$, was determined from $C_p'$ by using the partial specific volume of CA ($\bar{v}_2$), the specific volume of DMAc, and assuming additivity. $\bar{v}_2$ was measured pycnometrically at 25 and 50 °C. Since the difference between the two values was a small one, we used the value measured at 25 °C (0.723 mL/g) to calculate $v_2$ at all temperatures. To study the biphasic region, small samples (~2 mL) were subjected to extensive centrifugation (over 100 h) using a Beckman Spinco L 2 65 B ultracentrifuge at a rate of 28 000 rpm alternating rest and centrifugation periods.[1] Layers of the centrifugate were collected with a spatula and analyzed under the polarizing microscope. The temperature of transition cholesteric → isotropic transition, $T_{NI}$, was determined below room temperature by working in a cold chamber and at higher temperatures by using the hot stage of the microscope, noting the temperature at which

**Table II**
**Fractionation of Sample B**

| fraction | $\eta^{25}_{DMAc}$, dL/g | $\bar{M}_v$[a] |
|---|---|---|
| B I | 0.64 | 30 700 |
| B II | 0.77 | 38 400 |
| B III | 0.81 | 40 800 |
| B IV | 1.03 | 54 800 |
| B V | 1.07 | 57 000 |
| B VI | 1.15 | 62 700 |
| B VII | 1.77 | 106 000 |
| B VIII | 2.33 | 148 300 |
| B IX | 2.45 | 157 600 |
| B X | 2.46 | 158 400 |

[a] Using eq 2.

the field of observation darkened (under crossed polars for a solution at given $C_p$). $T_{NI}$ was confirmed by varying $C_p$ at constant temperature. $T_{NI}$ was preliminarily assessed by using heating rates of 10 °C/min. Henceforth, the heating rate in the interval $T_{NI}$ - 10 °C was lowered to 0.2 °C/min. Indetermination on $T_{NI}$ was estimated on the order of ±3 °C. Thermal transitions for undiluted B samples were also examined by DSC using a Perkin-Elmer DSC II instrument in an inert atmosphere. Samples were dried under vacuum at $T$ = 50 °C for 12 h or annealed under vacuum at 120 °C for 3 days. Heating rates were 40, 20, and 10 °C/min.

## Results and Discussion

**Viscosity and Light Scattering.** Molecular weights obtained from intrinsic viscosity by using eq 1–3 (respectively for samples A, B, and C) are included in Tables I and II. Light-scattering parameters ($\bar{M}_w$, virial coefficient $B$, and radius of gyration $\langle R_G^2 \rangle$) for samples A and B are also included in Table I. Light-scattering data were handled as described[3] in part 3 by plotting the quantity $Kc/R_\theta$ vs. the scattering-angle function $\sin^2 \theta/2$, or the polymer concentration $C$ in g/100 mL. The following equations hold

$$\lim_{\substack{C\to 0 \\ \theta \to 0}} \frac{Kc}{R_\theta} = \frac{1}{\bar{M}_w} + \frac{1}{\bar{M}_w} \frac{16\pi^2}{3\lambda^2} \langle R_G^2 \rangle \sin^2 \theta/2$$

$$K = \frac{2\pi^4 n^2 (dn/dc)^2}{N\lambda^4} \qquad (4)$$

$$R_\theta = \frac{r^2 I_\theta}{I_\theta (1 + \cos^2 \theta)}$$

where $\lambda$ is the wavelength, $n$ the refractive index, $N$ Avogadro's number, and $I_0$ and $I_\theta$ the incident and scattered intensity.

There is good agreement between the molecular weights obtained by viscosity and light scattering for sample B. When the differences between the DS of our sample A (Table I) and that of the samples used for deriving eq 1 (DS = 2.92) are considered, the difference in the molecular weight obtained with the two methods is not too large (use of eq 2 corresponding to DS = 2.46 would have yielded $\bar{M}_v$ = 170 000). Therefore, we felt that eq 2 could be used with confidence in deriving the molecular weight of sample B and its fractions.

Light-scattering plots in the concentration range up to $C \sim 0.7$ g/100 mL (Figure 1) exhibited a positive virial coefficient, reasonable radius of gyration (similar to that reported by Kamide et al.[12]), and no aggregation effects. However, when the concentration was above 1 g/100 mL, the $Kc/R_\theta$ vs. $\sin^2 \theta/2$ plot was no longer linear, and the $Kc/R_0$ vs. concentration plot revealed a maximum similar to that observed with some cellulose samples (Figure 4 of ref 3). Thus, association sets in even for CA when concentration exceeds 1 g/100 mL. To gain more information on the extent of the association, solutions were subjected to centrifugation at 19 500 rpm for lengths of time up to 7.5 h. Data in Figure 1 illustrate the $Kc/R_\theta$ vs. $\sin^2 \theta/2$ plot for a given sample having $C$ = 1 g/100 mL examined before and after centrifugation. The amount of material that was separated by centrifugation was practically undetectable, suggesting that very small amounts of associated species are responsible for the nonlinearity of the plots. When the centrifugated samples were allowed to rest undisturbed and hermetically closed for up to 2 weeks, the plots did not regain the characteristics observed before centrifugation, confirming the occurrence of only a slow and small association. The effect of centrifugation at other concentrations is shown by the $Kc/R_0$ vs. concentration plot in Figure 1.

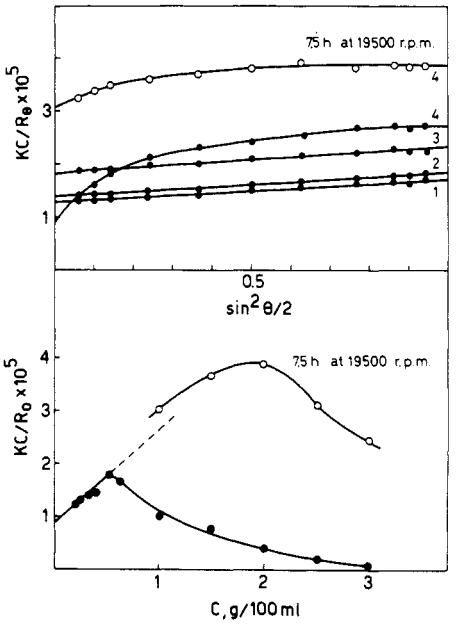


**Figure 1.** Light-scattering data for sample B in DMAc. (Top) Concentration is 0.26, 0.32, 0.52, 1.0 g/100 mL respectively for 1, 2, 3, 4. Solution 4 was reinvestigated following centrifugation for 7.5 h. (Bottom) The effect of centrifugation for 7.5 h on the data at $\theta$ = 0 is shown for concentrated solutions.

Viscosity–molecular weight–temperature data for sample B and its fractions are collected in Table III. The experimental points are superimposed to the theoretical $[\eta]$–$M$ curves in Figure 2 to evaluate the persistence length, $q$, at different temperatures. The theoretical curves are calculated by using the relationship of Yamakawa and Fujii[17] for unperturbed wormlike cylinders

$$[\eta] = \phi L'^{3/2}/\lambda^3 M \qquad (5)$$

where $L' = \lambda M/M_L$ is a reduced contour length ($M_L$ being the mass per unit length), $\lambda = 1/2q$, and $\phi$ is a function of $L'$ and of the reduced cylinder diameter $d'$ tabulated by Yamakawa and Fujii. $M_L$ was taken equal to 50.5 Da/Å, corresponding to a residue vector $L_0$ = 5.14 Å[18,19] and to a molecular weight of the repeating unit equal to 259 (DS = 2.30). The molecular diameter $d$ was taken equal to 8.1 Å, as obtained from the relationship[9]

$$d = (M_0/\rho N L_0)^{1/2} = (M_L/\rho N)^{1/2} \qquad (6)$$

where $\rho$, the density of both diacetate and triacetate, = 1.3 g/cm$^3$, in agreement with data in the literature.[9,20] The experimental points in Figure 2 (left) suggest that at 25 °C $q$ = 70 Å. Values obtained at other temperatures are collected in Table IV. The errors and the limitations attending the use of eq 5 for the evaluation of $q$ have been

**Table III**
**Viscosity–Temperature Data for Fractions of Sample B (DS = 2.3) in DMAc**

| sample/$\bar{M}_v$ | $[\eta]_{DMAc}$, dL/g | | | |
|---|---|---|---|---|
| | 25 °C | 50 °C | 70 °C | 110 °C |
| B IV/54 800 | 1.03 | 0.88 | 0.81 | 0.61 |
| B VI/62 700 | 1.15 | 0.94 | 0.82 | 0.64 |
| B/115 600 | 1.90 | 1.60 | 1.37 | 1.00 |
| B VIII/148 300 | 2.33 | 2.00 | 1.72 | 1.26 |

**Table IV**
**Temperature Variation of Axial Ratio and $\nu_2'$ for CA with DS = 2.3**

| $T$, °C | $q$, Å | $x = 2q/d$[a] | $\nu_2'$ theor[b] | $\nu_2'$ exptl[c] |
|---|---|---|---|---|
| 25 | 70 | 17.3 | 0.41 | 0.33 |
| 50 | 56 | 13.8 | 0.495 | 0.37 |
| 70 | 48 | 11.8 | 0.561 | 0.41 |
| 110 | 36 | 8.9 | 0.698 | 0.55 |

[a] $d$ = 8.1 Å, eq 6. [b] From eq 8. [c] Interpolated from data in Figure 3.

discussed in the preceding papers.[1,2,4] In particular, excluded-volume effects are quite small for CA in DMAc.[21] $q$ appears to decrease with temperature.

Also included in Figure 2 are the data of Kamide et al. for a diacetate[14] (DS = 2.46) at 25 °C (left) and a triacetate[13] (DS = 2.92) at 25 °C (right), both in DMAc. For the latter plot, the $M_L$ value used was 55.4, corresponding to $M_0$ = 285 and $L_0$ = 5.14 Å. $d$, from eq 6, was 8.3 Å. The latter data indicate $q \sim 65$ Å for the triacetate.

The results show that the persistence length of CA at 25 °C is comparable to that of HPC[1,2] in DMAc (~70 Å) and smaller than that observed for HPC in DCA (~100 Å)[2] and for cellulose. For the latter, we reported[4] a value of ~110 Å in DMAc/LiCl. Since $q$ for the triacetate is only slightly smaller than for the diacetate, the conformations of HPC and CA in DMAc should be similar. It is not simple to compare the conformations of CA and cellulose due to the need of using LiCl to dissolve the latter. Saito[16,21] concluded that the unperturbed radius of gyration of CA in DMAc increases between DS = 0.49 and 2.46 and greatly decreases at DS = 2.92. Again, we are puzzled by the fact that we were unable to dissolve CA with DS = 0.9 in pure DMAc.

The persistence length of sample B can also be derived from the light-scattering data in Table I. The coil limit of $q$ is defined as

$$q_{CL} = 3\langle R_G^2\rangle / L \qquad (7)$$

where the contour length, $L$, is $(M_w/M_0) \times 5.14$. Equation 7 yields $q_{CL}$ = 140 Å, which is about a factor of 2 greater than $q$ derived from the Yamakawa–Fujii theory ($q_{YF}$). Conversion of the measured $Z$-average value of $\langle R_G^2\rangle$ into a weight-average value[16] would lower $q_{CL}$ by about 40%. Saito[21] also reports that $q_{YF}$ is smaller, by about a factor of 2, than $q_{CL}$. Numerically his values of $q_{YF}$ and $q_{CL}$ are similar to ours. Since CA appears to be close to gaussian behavior, he attributes the difference between $q_{YF}$ and $q_{CL}$ to the neglect of a draining term[22] in the YF theory. A draining effect was in fact evidenced by the hydrodynamic data for CA.[16,21] We note that for HPC we observed $q_{YF} \sim q_{CL}$. An additional parameter that affects the value of $q_{YF}$ is the diameter of the unperturbed cylinder. For consistency with our results for HPC and cellulose we have used the unsolvated diameter (8.1 Å) from eq 6. However, with a rather complex calculation that probably entails considerable error, Saito derives an hydrodynamic diameter $d_h$ which is on the order of 30 Å. Such a revision would lower our $q_{YF}$ value to 47 Å.

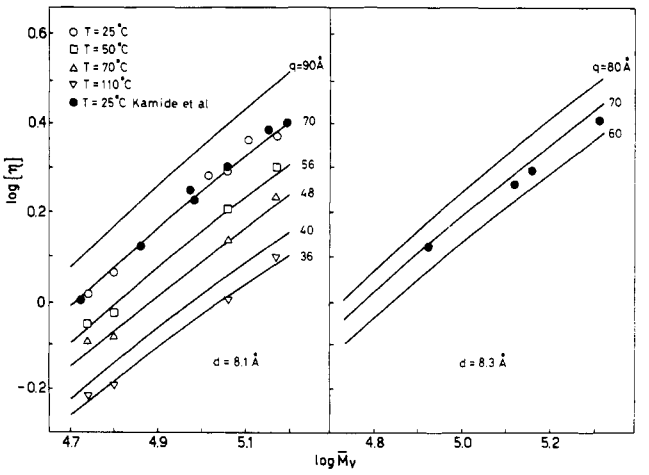


**Figure 2.** (Left) Full lines represent the theoretical[17] intrinsic viscosity–molecular weight dependence for the indicated values of $q$, $M_L$ = 50.5 Da/Å, and $d$ = 8.1 Å. Open points: experimental values for CA with DS = 2.3 (Table III) in DMAc. Filled points: experimental points at 25 °C from Kamide et al.[11] (Right) Similar plot for the triacetate (DS = 2.92) with $d$ = 8.3 Å and $M_L$ = 55.4 Da/Å using the experimental values of Kamide et al.[12] at 25 °C.

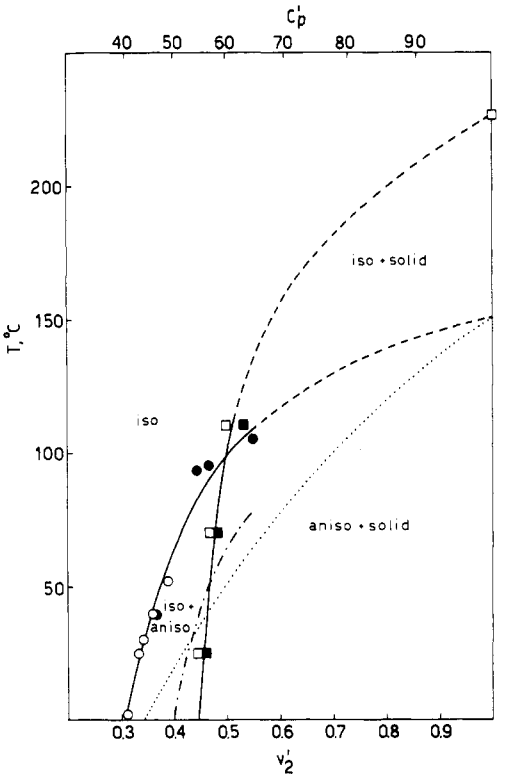


**Figure 3.** Phase diagram for CA sample B: (○, ●) isotropic → anisotropic ($C_p'$ or $\nu_2'$); (□, ■) isotropic or anisotropic → solid; (···) eq 28–30 of ref 29; (···) hypothetical position of the $C_p''$ ($\nu_2''$) boundary if $C_p''/C_p' = 1.25$.

**Phase Equilibria. Solubility/Melting.** Solubility data for samples A–C are collected in Table V. For sample B, data obtained at different temperatures are included in the phase diagram in Figure 3 (□ indicates a solution just before the solid appears, ■ the solution in the presence of a small amount of solid). Solutions of samples A and C were invariably isotropic up to the solubility limit. Solutions of B, and of its fractions, crystallized out of an anisotropic solution up to ~100 °C. The solubility of sample C, measured with a small amount (~0.06%) of LiCl, was extremely low. A DSC scan for fraction BI is illustrated in Figure 4. The peak of the endotherm is at 223 °C, and the cooling curve suggests an undercooling of

Table V
Solubility Data

| sample/solvent | T, °C | solubility %, w/w |
|---|---|---|
| A/DMAc | 25 | 25 |
| B/DMAc | 25 | 55 |
| B/DMAc | 70 | 57 |
| B/DMAc | 105 | 61.5 |
| B II/DMAc | 25 | 60 |
| C/DMAc + 3% LiCl | 25 | 8 |
| C/DMAc + 0.06% LiCl | 25 | 0.1 |

~20 °C. Observation under the polarizing microscope at these temperatures reveals a bright field at ~218 °C, but no flow ability, and a complete isotropization at ~226 °C. On the basis of this evidence, and also on the temperature dependence of $q$ and $v_2'$ (cf. seq.), we attribute the endotherm at 223 °C to a crystal → isotropic transition. Accordingly, the solubility line in Figure 3 is extrapolated to $T_{CI}^0$ = 223 °C.

**Mesophase.** The variation of the critical concentration ($C_p'$) and volume fraction ($v_2'$) with temperature between 2 and 105 °C for sample B is illustrated in Figure 3 (○ indicates result obtained by increasing $C_p$ at constant $T$, ● indicates increasing $T$ at constant $C_p$). Accounting for the exact variation of $v_2'$ with $T$ due to thermal expansion would entail a correction of ~0.01 on each point in Figure 3. The occurrence of a biphasic region could not be evidenced for sample B due to the difficulty in separating the extremely viscous phases even after extensive centrifugation. We were, however, able to demonstrate the occurrence of a biphasic region working with the less viscous B III fraction at a concentration $C_p$ = 43.4%. Upon extensive centrifugation (see Experimental Section), the upper layer was completely isotropic while the intermediate and bottom layers were birefringent. Upon standing for 4–5 h following centrifugation, the intermediate layer revealed typical nematic (cholesteric) droplets dispersed in an isotropic liquid (Figure 5). Cholesteric colors were observed when the samples were allowed to rest for ~3 months. In view of the problems in separating the two phases, the determination of the conjugate $C_p''$ concentration becomes an almost impossible task. We have therefore assumed $C_p''/C_p' = 1.25$, similar to the ratio determined for HPC in DMAc, and plotted the deduced $C_p''$ vs. $T$ on the phase diagram in Figure 3. The diagram reveals that the solubility line is rather close to the biphasic gap; actually only solutions below ~50 °C may exhibit stable anisotropy. At higher temperatures the solubility line encroaches the biphasic gap, and the cholesteric solution can be observed only under nonequilibrium conditions. The latter situation was observed with cellulose[4] and has been discussed by Papkov,[23] Balbi et al.,[24] and Ciferri and Krigbaum.[25]

The isothermal variation of $v_2'$ with molecular weight is illustrated in Figure 6, which also includes the variation of solubility with molecular weight. The data at 21 °C are collected in Table VI. As observed with HPC[1,2] and with cellulose,[4] $v_2'$ decreases with molecular weight and tends to an asymptotic value. The asymptote is $v_2' \sim 0.33$, remarkably close to the value of 0.35 observed[2] for HPC in DMAc which has a persistence length similar to that of CA.

**Comparison with Theory.** In Figure 6 the asymptotic limit of the $v_2'$ is compared with the prediction of the lattice theory for a semirigid Kuhn chain[26]

$$v_2' = \frac{8}{X_K}\left(1 - \frac{2}{X_K}\right) \qquad (8)$$

where $X_K$ is the axial ratio of the Kuhn segment equal to

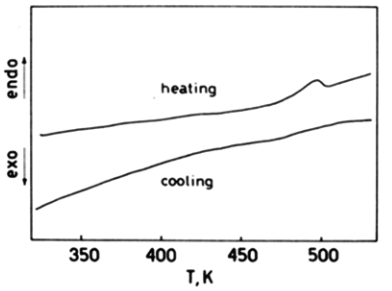


**Figure 4.** DSC thermogram for fraction BI annelaed at 120 °C. Heating rate is 10 °C/min; 3.7 mg.

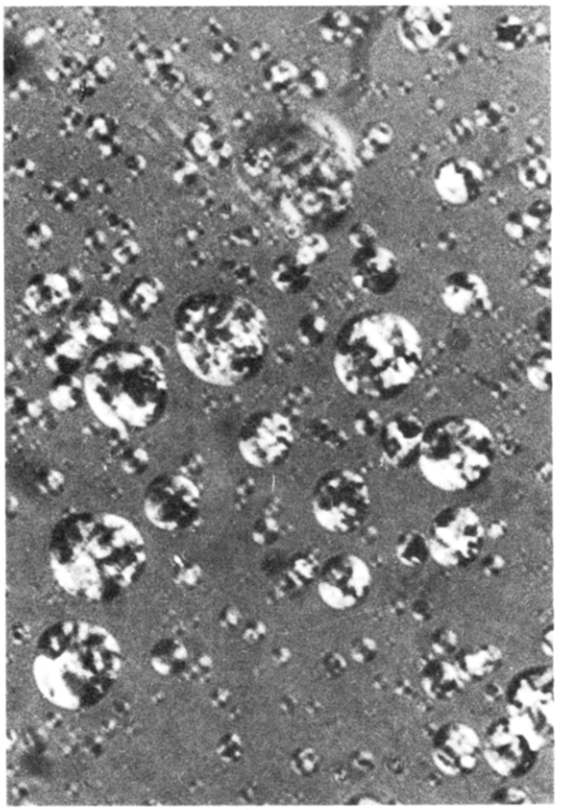

**Figure 5.** Micrograph of sample B III centrifugated at 28 000 rpm for ~100 h.

$2q/d$. As was the case with HPC/DMAc, HPC/DCA, and cellulose/DMAc + LiCl, the occurrence of an asymptotic behavior is in line with theory, but the theoretical value of $v_2'$ is somewhat larger than the experimental one. Table VII summarizes the results for the present and the previously investigated systems. For consistency we use persistence lengths obtained from the Yamakawa–Fujii theory and diameters obtained from eq 6. We do not discuss theoretical formulations for rigid and wormlike chains,[27] since, as previously discussed,[1,2,4] eq 8 offers the closest representation of the asymptotic behavior. The data in Table VII are also plotted in Figure 7 as $v_2'$ vs. $q$, and $v_2'$ vs. $4d/q$, a form suggested by the approximation $v_2' \sim 8/X_K$.

When an ensemble of data such as that presented in Table VII is considered, it is evident that $v_2'$ is definitively correlated with a molecular parameter which describes chain rigidity. The functional dependence of eq 8 is also a satisfactory representation of the data. In spite of these successful features of the theory, the experimental value of $v_2'$ is *systematically* smaller than expected from eq 8. At least three reasons can be considered to justify the difficulty in predicting the absolute value of $v_2'$. First, the value of $X_K$ is affected by the indetermination on the value

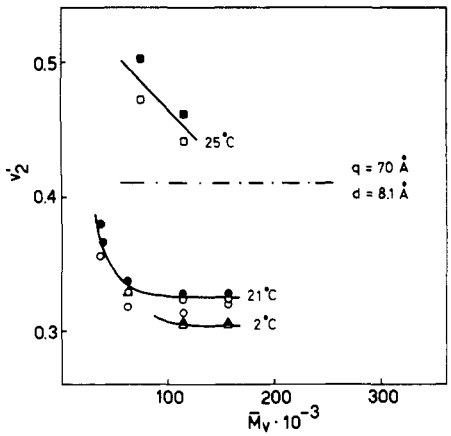


**Figure 6.** Variation of $\nu_2'$ at 2 and 21 °C and of solubility (□, ■) at 25 °C, with MW for fractions of sample B. (---): eq 8.

**Table VI**
**Critical Compositions of CA Fractions at 21 °C**

| sample/$\bar{M}_v$ | $C_p'$ | $\nu_2'$ | appearance |
|---|---|---|---|
| B II/38 400 | 45.0 | 0.356 | isotropic |
| | 47.6 | 0.381 | isotropic + anisotropic |
| B III/40 500 | 46.2 | 0.367 | isotropic + anisotropic |
| B VI/62 700 | 42.0 | 0.329 | isotropic |
| | 42.6 | 0.334 | isotropic + anisotropic |
| B/115 600 | 41.6 | 0.325 | isotropic |
| | 41.9 | 0.328 | isotropic + anisotropic |
| B X/158 400 | 41.5 | 0.324 | isotropic |
| | 41.9 | 0.328 | isotropic + anisotropic |

**Table VII**
**Summary of Persistence Length and $\nu_2'$ Values at Room Temperature**

| system | $q_{YF}$, Å | $\nu_2'$, exptl | $\nu_2'$ (eq 8) | $d$ (eq 6), Å |
|---|---|---|---|---|
| HPC/DMAc (ref 1) | 70 | 0.35 | 0.59 | 10.4 |
| HPC/DCA (ref 2) | 100 | 0.15 | 0.34 | 10.4 |
| cellulose/DMAc + 5% LiCl (ref 4) | 110 | 0.06 | 0.18 | 5.8 |
| CA/DMAc (present) | 70 | 0.33 | 0.41 | 8.1 |

of $q$ (which may not be satisfactorily identified with $q_{YF}$) and $d$ (the latter also affects the value of $q_{YF}$). These effects have been discussed above and in the preceding articles.[1,2,4] Secondly, soft interactions[28] may occur and, as described in parts 1, 2, and 4, their inclusion in the theory could lower the value of $\nu_2'$ calculated by using eq 8. It was shown that a value of the parameter $T^*$ (which characterizes the strength of soft interactions) between 75 and 150 K would assure agreement between theory and experiment for the limiting value of $\nu_2'$. A somewhat smaller value of $T^*$ (~70) would be required in the case of the CA/DMAc system, which exhibits the smallest deviation between experimental and theoretical values of $\nu_2'$ (Table VII). $T^*$ could be independently evaluated[9] to ascertain whether or not soft interactions are indeed occurring.

The third possible reason for the discrepancy in the $\nu_2'$ values could arise from molecular association. The problem has been discussed in detail for cellulose[4] when significant aggregation and association phenomena were detected.[3] Since some association was also evidenced for the present CA/DMAc system, the question arises of whether association is actually a general phenomenon, which would make the interpretation of $\nu_2'$ in terms of molecular parameters an almost impossible task.[4] We feel that the data in Figure 7, as well as the correlation between the temperature dependencies of $\nu_2'$ and of the persistence length (cf. seq.), offer compelling evidence for a direct role of

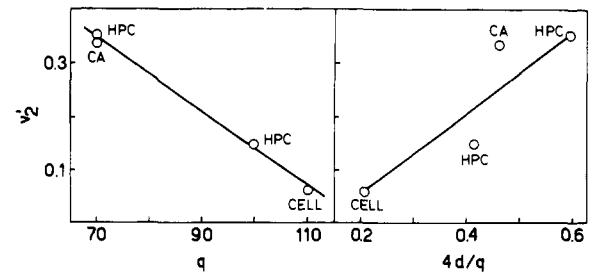


**Figure 7.** Experimental value of $\nu_2'$ for several polymer/solvent systems (Table VII) plotted vs. $q$ or $4d/q$.

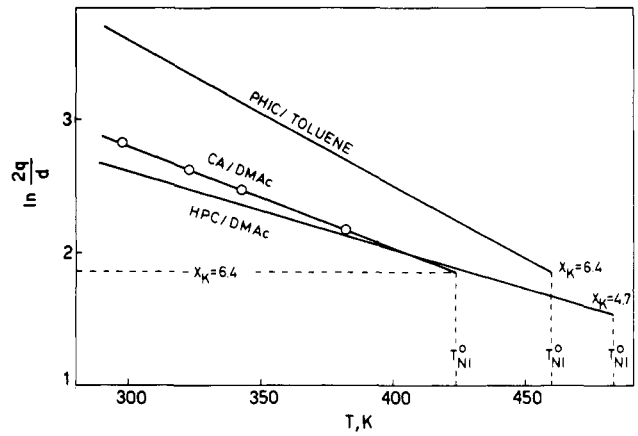


**Figure 8.** Variation of the axial ratio of the Kuhn segment with temperature for CA/DMAc, HPC/DMAc,[2] poly(*n*-hexyl isocyanate) (PHIC)/toluene.[29]

molecular rigidity on the critical composition. It just would be too fortuitous that associated species had axial ratios, and temperature dependence of axial ratios, similar to those corresponding to the values of $q$ and $dq/dT$ measured in diluted solutions for a wide variety of polymer/diluent systems. As the present light-scattering results suggest, the concentration of associated species might be negligeable, with the possible exception of the cellulose/DMAc + LiCl system.

Finally, a correlation between the thermotropic effect (i.e., the temperature variation of $\nu_2'$) and the temperature variation of $q$ is exhibited by the present system in analogy to the HPC/DMAc[1,2] and other systems.[29] By the use of the data in Table IV, ln $(2q/d)$ is plotted vs. $T$ in Figure 8. Data for other systems are included. The quantity $d \ln (2q/d)/dT$ is $\sim -7.8 \times 10^{-3}$ deg$^{-1}$, and the temperature at which $2q/d$ attains the critical value[9] 6.4 is ~150 °C. We have shown[2,29] that this temperature must be very close to the nematic → isotropic transition temperature, $T_{NI}^0$, for the net liquid crystal. We note that $T$ = 150 °C, being below $T_{CI}^0$ = 223 °C, would correspond to $T_{NI}^0$ if the solubility line did not cross the $\nu_2'$ vs. $T$ curve (see Figure 3). A correlation between $d(2q/d)/dT$ and $d\nu_2'/dT$ is given by Krigbaum et al.[29] (cf. 28–30 of ref 29). Use of these relationships, with the assumption $T_{NI}^0$ = 150 °C, produces the dotted line in Figure 3. The latter offers a satisfactory theoretical description of the experimental variation of $\nu_2'$ with $T$. Residual deviations between theory and experiments are similar to those observed in ref 29.

Recently Ronca and Yoon have presented a theory for semiflexible chains based on the wormlike model with a limiting curvature.[30] This theory predicts absolute stability of the mesophase ($T_{NI}^0 = \infty$) for chains of adequate persistence and contour length, and values of $T$ ($d \ln \langle r^2 \rangle / dT$) not greater than −1. This limit is clearly exceeded by the present data, as well as by the data for other cellulosic

derivatives[1,2] and poly(*n*-hexyl isocyanate).[29]

**Acknowledgment.** We express our appreciation to Prof. G. Torri for the NMR determinations. This investigation has been supported by the Italian Research Council through its "Chimica Fine e Secondaria" project.

**Registry No.** CA, 9004-35-7; DMAc, 127-19-5.

## References and Notes

(1) Conio, G.; Bianchi, E.; Ciferri, A.; Tealdi, A.; Aden, M. A. *Macromolecules* **1983**, *16*, 1264.
(2) Aden, M. A.; Bianchi, E.; Ciferri, A.; Conio, G.; Tealdi, A. *Ibid.* **1984**, *17*, 2010.
(3) Terbojevich, M.; Cosani, A.; Conio, G.; Ciferri, A.; Bianchi, E. *Ibid.* **1985**, *18*, 640.
(4) Bianchi, E.; Ciferri, A.; Conio, G.; Cosani, A.; Terbojevich, M. *Ibid.* **1985**, *18*, 646.
(5) Meeten, G. H.; Navard, P. *Polymer* **1983**, *24*, 815.
(6) Marsano, E.; Bianchi, E.; Ciferri, A. *Macromolecules* **1984**, *17*, 2886.
(7) Dayan, S.; Maissa, P.; Vellutini, P.; Sixou, P. *J. Polym. Sci., Polym. Lett. Ed.* **1982**, *20*, 33.
(8) Flory, P. J. *Proc. R. Soc. London, A.* **1956**, *234*, 60.
(9) Flory, P. J. *Adv. Polym. Sci.* **1984**, *59*, 1.
(10) Patel, D. L.; Gilbert, R. D. *J. Polym. Sci., Polym. Phys. Ed.* **1983**, *21*, 1079.
(11) Kamide, K.; Miyazaki, Y.; Abe, T. *Polym. J. (Tokyo)* **1979**, *11*, 523. Kamide, K.; Terakawa, T.; Miazaki, Y. *Ibid.* **1979**, *11*, 285.
(12) Kamide, K.; Saito, M. *Ibid.* **1982**, *14*, 517.
(13) Goodlett, V. W.; Dougherty, J. T.; Patton, H. W. *J. Polym. Sci., Polym. Chem. Ed.* **1971**, *9*, 155.
(14) ASTM D-871-56 (ASTM Standards 1958, Part 8 Lacquers and Lacquer Materials, p 460).
(15) Kamide, K.; Saito, M.; Abe, T. *Polym. J. (Tokyo)* **1981**, *13*, 421.
(16) Saito, M. *Ibid.* **1983**, *15*, 249.
(17) Yamakawa, H.; Fujii, M. *Macromolecules* **1974**, *7*, 128.
(18) Brant, D. A.; Goebel, K. D. *Ibid.* **1972**, *5*, 536.
(19) Marchessault, R. M.; Sarko, A. *Adv. Carbohydr. Chem.* **1967**, *22*, 421.
(20) Panar, M.; Wilcok, O. B. Ger. Offen. 2705382, Aug 11, 1977. Fr. Demande 77, 3473, 1977 (to the Du Pont Co.).
(21) Saito, M. *Polym. J. (Tokyo)* **1983**, *15*, 213.
(22) Kirkwood, J.; Riseman, J. R. *J. Chem. Phys.* **1948**, *16*, 565.
(23) Papkov, S. *Contemp. Top. Polym. Sci.* **1977**, *2*.
(24) Balbi, C.; Bianchi, E.; Ciferri, A.; Tealdi, A.; Krigbaum, W. R. *J. Polym. Sci., Polym. Phys. Ed.* **1980**, *18*, 2037.
(25) Ciferri, A.; Krigbaum, W. R. *Mol. Cryst. Liq. Cryst.* **1981**, *69*, 273.
(26) Flory, P. J. *Macromolecules* **1978**, *11*, 1141.
(27) Khokhlov, A. R. Semenov, A. N. *Physica A* **1982**, *112A*, 605.
(28) Warner, M.; Flory, P. J. *J. Chem. Phys.* **1980**, *73*, 6327.
(29) Krigbaum, W. R.; Hakemi, M.; Ciferri, A.; Conio, G. *Macromolecules* **1985**, *18*, 973.
(30) Ronca, G.; Yoon, D. Y. *J. Chem. Phys.* **1985**, *83*, 373.

# Phase Structure of Lamellar Crystalline Polyethylene by Solid-State High-Resolution $^{13}C$ NMR: Detection of the Crystalline–Amorphous Interphase

**Ryozo Kitamaru,* Fumitaka Horii, and Kouichi Murayama**

*Institute for Chemical Research, Kyoto University, Uji City, Kyoto 611, Japan.*
*Received June 5, 1985*

ABSTRACT: The phase structure of lamellar crystalline polyethylene is investigated in detail by high-resolution solid-state $^{13}C$ NMR, utilizing different pulse sequences for spectrum detections. It is concluded that samples crystallized from the melt consist of the lamellar crystalline phase, a crystalline–amorphous interphase, and an isotropic amorphous phase, whereas samples crystallized from dilute solution consist of the lamellar crystalline phase and a noncrystalline overlayer. These component phases are explicitly characterized in terms of the chemical shift and the spin–lattice and spin–spin relaxation times.

## Introduction

Lamellar crystalline polyethylene contains a noncrystalline part to some extent, whether it is crystallized from the melt or from dilute solution. A question arises as to whether this noncrystalline content is in a disordered amorphous state or in any particular ordered state due to the coexistence of lamellar crystallites. This problem has been extensively studied for several decades. It has been found by $^1H$ broad-line NMR investigations that samples crystallized from the melt (hereafter referred to as bulk crystals) generally consist of three regions: the crystalline region with molecular chains oriented perpendicular to the wide faces of the lamella, the noncrystalline interfacial region with limited molecular mobility, and the noncrystalline interzonal region with liquidlike molecular mobility.[1-5] Polyethylene samples crystallized from dilute solution (hereafter referred to as solution crystals) consist of lamellar crystals and noncrystalline overlayers with a negligibly small amount of noncrystalline interzonal material with pronounced molecular mobility.[2-4]

It has also been found that both bulk crystals and solution crystals contain a noncrystalline part that can be detected by $^1H$ scalar-decoupled $^{13}C$ NMR.[6,7] The $^{13}C$ spin–lattice relaxation time $T_{1C}$ is almost the same at room temperature for the two series of samples, whereas the spin–spin relaxation time $T_{2C}$ of the solution crystals is much shorter than that of the bulk crystals. Therefore, one can assume that the noncrystalline overlayer in solution crystals does not consist of regularly folded methylene sequences connecting adjacent crystalline sequences; such an overlayer must comprise methylene sequences randomly connecting crystalline sequences. The molecular chains forming the noncrystalline overlayer can execute local molecular motion, as suggested by $T_{1C}$ being equal to that of the noncrystalline interzonal material in the bulk crystals, but the chain motion and the long-range conformation are restricted as shown by the very short $T_{2C}$.

However, an objection was raised concerning our $^1H$ broad-line spectrum analysis: the contribution from the noncrystalline material in the polyethylene samples should not be analyzed in terms of two components, as done in ref 1–4, but should be treated as one component.[8] Until now we were not in a position to respond to this criticism, since $^1H$ broad-line NMR spectroscopy is not sensitive enough to solve this problem. We report here evidence of the presence of two kinds of noncrystalline components. Moreover, we had previously no firm evidence that all of the noncrystalline components in the samples studied were detected by the above-mentioned $^1H$ scalar-decoupled $^{13}C$ NMR spectroscopy. The application of solid-state high-

0024-9297/86/2219-0636$01.50/0 